Influence of Parasitic Capacitances of IGBT Inverter on Insulation Condition Monitoring of Traction Machines Based on Current Signal Transients Analysis

C. Zoeller[1], M.A.Vogelsberger[2] and T.M.Wolbank[1]
[1]TU Wien - Institute of Energy Systems and Electrical Drives
Gusshausstr. 25-29 / 370-2 1040 Vienna, Austria
Tel.: +43 (1) – 58801 370226
Fax: +43 (1) – 58801 9370226
E-mail: thomas.wolbank@tuwien.ac.at
[2]Bombardier Transportation Austria

Acknowledgements

The work to this investigation was supported by the Austrian Research Promotion Agency (FFG) under project number 838478. The authors want to thank Bombardier Transportation Mr. D. Baro and Mr. M. Bazant Product Development ISC_M-Drives for product development funding and the great support. Thank also goes to Mr. Markus Jörg (Head ISC_P_Co2E; Zürich) for his great feedback regarding converter topic and overlay project supervision.

Keywords

AC machine, Electric breakdown, Fault detection, Insulation testing, Pulse width modulation inverters

Abstract

At inverter-fed traction drives stray currents due to parasitic capacitances in frequency converters and machine cause high frequency voltage components spreading into all conductive components of the drive system. These hf voltages are harmful and origin from the inverter side through fast switching power semiconductors with high levels of output voltage steepness. Additionally overvoltage at the machine occurs by inverter operation of the machine and is thus stressing the machine insulation system. These effects can lead to a reduction of the machine insulation lifetime due to loss of insulation strength. Thus, insulation condition monitoring systems are necessary to enable a safe and reliable operation of a drive. Insulation condition monitoring of inverter-fed traction drives is implemented in this work by evaluating the transient current response after voltage step excitation. The current measurement is performed using the built-in current transducers of the inverter, normally used for the control of the drive, to save cost and space. Insulation degradation usually is a slowly developing process, at which the parasitic capacitances of the winding system change and thus also the transient current response. However, influences from the inverter capacitances cannot be neglected and thus the influence of the parasitic capacitances located in the inverter on the proposed insulation condition monitoring is investigated.

Introduction

The electrical winding insulation of rotating machines is one of the most important parts, although it is often seen only as ballast that delivers no share on the energy conversion inside the machine. However, a weak insulation system could not guarantee the continuous operation without outage even over decades. The strength of the insulation is gradually degraded during operation of the drive through different combined stresses, e.g. thermal, electrical, mechanical and environmental influences, as described in [1]. Today's estimation of the insulation condition and the remaining lifetime of the insulation of a machine is evaluated with empirical methods based on extensive tests and dielectric measurements, like dissipation factor [2], capacitance and insulation resistance measurements [3],

which deliver integral diagnostic of the insulation strength. With the partial discharge test locally limited defects can be investigated [4]-[5]. Especially the last mentioned test procedure often demands the experience of the examiner. Different approaches regarding the condition monitoring are described in [6]-[7].

The insulation degradation process is usually slowly developing, first starting with the deterioration of the turn-turn insulation and finally leading to higher severity faults like phase to phase or phase to ground, respectively that leads to a breakdown of the insulation. In [8] and [9] tests with accelerated insulation aging conducted with thermal exposure cycles on stator coils show that the parameter which is mainly influenced by the changes of the material is the insulation capacitance. The capacitance values of all specimens have changed over times and with the number of aging cycles. These effects can be observed at high voltage tests with several time of the nominal voltage [8] as well as at low voltage tests over a wide frequency range [10]. The capacitance is in all cases usually considered as the dominant parameter for insulation health state evaluation.

Modern voltage source inverters (VSI) with fast switching transitions in today's traction drive applications lead to transient overvoltage, stressing the machine's insulation system. Additionally new emerging semiconductor technologies with high switching frequencies and high dv/dt-rates increase the stress for the motor winding insulation [11]. This leads to insulation deterioration and accelerated loss of the electrical strength of the system, which finally results in an insulation breakdown. To increase the reliability of the drive system different strategies like fault tolerant design, electrical filters etc. can be implemented. However, filters are bulky, increase space requirements and lead to additional costs. With the proposed method, the inverter is able to analyze the insulation state of the machine using the integrated current sensors for machine control. Thus unexpected down times can be avoided and maintenance on demand scheduled.

In this paper, a method for monitoring the insulation state in a drive system based on evaluation of the transient current signal after inverter switching is presented. By evaluation of the occurring frequency components in the transient current response, a correlation to a change in the insulation strength can be shown. Experimental results of this concept tested at a 1.4MW induction machine for railway application are presented and show the applicability of the method. Further, the influence of the parasitic capacitances of the inverter is analyzed.

Transient Current Response for Insulation Condition Evaluation

In Fig. 1 the scheme of the inverter-cabling-machine arrangement of the test bench is shown. The figure illustrates the measurement procedure by applying a voltage step with the inverter from lower short circuit to high DC-link voltage in phase L1. The procedure is repeated for every phase separately. The measurements were conducted at stand still without magnetization of the machine and could be implemented as a startup routine before operation of the drive. A voltage step applied with the inverter elicits a response in the system influenced by the parameters of each system-component. Also the parasitic components affect the response of the system. At the cabling, the phase-to-phase and phase-to-ground parasitic capacitances ($C_{Ph\text{-}Ph}$, $C_{Ph\text{-}Gnd}$) are considered as well as inside the motor the parasitic winding capacitances, i.e., $C_{Ph\text{-}Gnd}$, $C_{Ph\text{-}Ph}$ and $C_{Turn\text{-}Turn}$ are included which largely influence the high frequency behavior and consequently the transient overvoltages at the machine after inverter switching with steep voltage rise. Furthermore, on the inverter side, the internal capacitances of the semiconductor modules and the capacitive coupling to ground $C_{Inv\text{-}Gnd}$ are indicated. Additionally, the inverter contains a monitoring unit of the collector-emitter voltage in the switched-on state. Through the V_{CE} monitoring, implemented with a specific driver module and the external calculated components R_{VCE} and C_{VCE}, it has the ability to detect short circuits very quickly and turn off the IGBT in this case by a specially slow turn-off (soft turn off) without damage caused by surges.

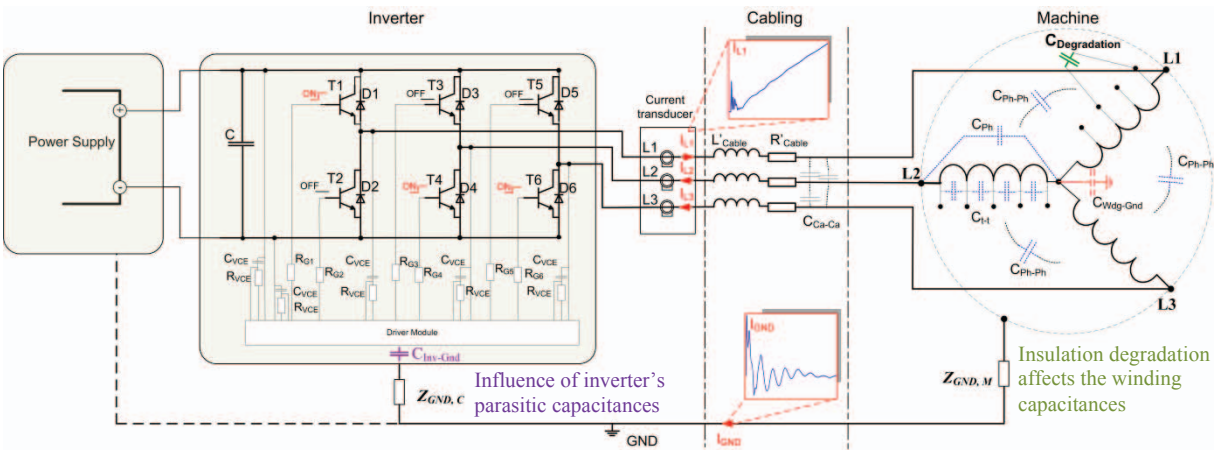

Fig. 1 Scheme of the test stand with inverter, cabling and the machine

In Fig. 2, the current response as a reaction of a switching transition of the inverter, measured on phase L1 is depicted for two different machine states, first the healthy machine and second the same machine with a capacitor placed parallel to the first coil of phase L1. Due to the aforementioned investigations showing that a change in the winding capacitance occurs at insulation deterioration of the winding system, the degradation of the insulation system in this work is emulated with capacitors having different values placed parallel to the winding system. Therefore, the test machine is equipped with fiber-insulation wires and additional taps accessible at terminal connection block. Different degradation scenarios can thus be analyzed by varying the position and size of the capacitors (variation of '$C_{Degradation}$' in a range from 1nF to 15nF). The capacitance value of the whole winding system of the test machine (1.4 MW induction machine) measured to ground is about 63nF.

With the simplified assumption that the recorded signal $i(t)$ after a voltage step excitation is a superposition of a linear current slope, defined by the inductance of the machine and a transient portion i_{trans}, the trace can be described by the equation $i(t) \approx 1/L \int_{-\infty}^{t} u(\tau)d\tau + i_{trans}(t)$. The oscillation of i_{trans} decays after some ten microseconds and afterwards follows the typical inductive behavior, depending also on inherent machine asymmetries, e.g. slotting or saturation, which contains no significant information for the insulation state estimation. This inductive part is eliminated by subtraction of the mean current slope. The characteristics of the deviation in the shape of the first transient part are analyzed in the frequency domain. After the accurate switching time point has been determined, the time domain data is transformed using Fourier analysis into the frequency domain (cf. Fig. 2b).

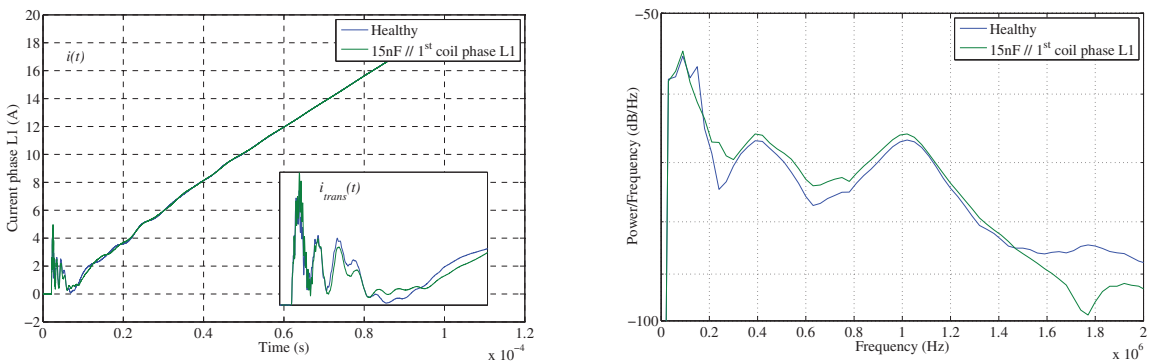

Fig. 2 a) current response for two different machine insulation conditions b) Spectra of transient current responses

The difference of the spectra of the two investigated machine states is depicted in Fig. 2 (b) for a frequency range up to 2 MHz. The affected frequency range depends on the size of the machine and

position of the fault capacitor. Based on the root mean square deviation between the 'Healthy' and 'Degraded -15nF // 1st coil phase L1' trace for every equidistant frequency point within a defined frequency range an indicator (Insulation State Indicator) ISI is calculated to assess the severity of the insulation degradation. In [12] a detailed description of the ISI calculation is given. On the basis of the trend of the indicators over time, insulation deterioration can be concluded and further maintenance steps scheduled.

Fig. 3 depicts the values of the ISI indicator for different machine states, at which different capacitors are placed in parallel to the first coil of phase L1 to emulate initial and ongoing insulation degradation at an early stage. The bar chart of Fig. 3 represents the indicators in graphical form. A monotonic increase of the indicators with increasing capacitor values is observable.

TABLE 1 RESULTS OF THE INDICATORS FOR MACHINE SCENARIOS

Machine State	ISI value
Healthy	$1.94*10^{-3}$
1.5nF // 1st coil Phase L1	$4.681*10^{-3}$
3nF // 1st coil Phase L1	$6.736*10^{-3}$
15nF // 1st coil Phase L1	$16.831*10^{-3}$

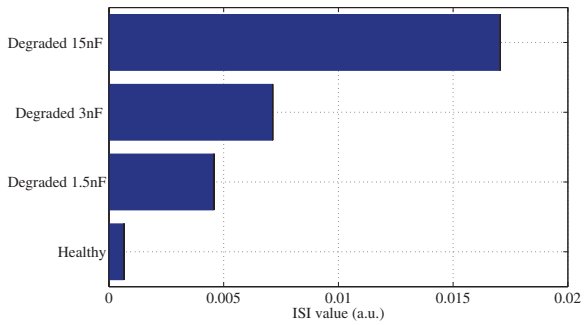

Fig. 3 Representation of the indicators

In previous works the influence of the machine's parasitic capacitances on the transient current response after step excitation is analyzed more in detail in [8]. Investigations regarding the cabling parameters and their influence on the method are described in [12] by separating the affected frequency ranges and excluding it in the observed frequency range. The next section deals with the influence from the inverter and its parasitic capacitances.

Influence of Inverter Parasitic Capacitances

The usage of frequency converters in traction drives are accompanied by undesirable high frequency effects in the power electronic as well as in the machine. Stray currents due to parasitic capacitances cause high frequency voltage components spreading into all conductive components of the drive system. Fast switching power semiconductors with high levels of output voltage steepness (dv/dt) cause overvoltages through reflection phenomena, resonance oscillations within the winding system and non-linear voltage distributions [13]-[14]. With accelerated rate of change in trends of power electronic devices and upcoming new semiconductor technologies (SiC, GaN), these effects will intensify.

This chapter deals with the influence of the parasitic capacitances of the inverter. The accurate identification of the parasitic parameters of all drive components is one of the most difficult problems, especially in the hf range. These capacitances induce various effects such as harmful common mode CM currents or resonances in parasitic sub circuits [15]-[16]. As aforementioned in the introduction a step input introduced by the PWM waveform in a power drive system elicits a response in the system. When subjected to a high dv/dt voltage rise, all parasitic components interact with each other and produce ringing. As the power components of the inverter also may deteriorate over time, their internal parasitic elements also age. Furthermore, a change by an exchange of an inverter component should also be evoked. In Fig. 4 the inverters internal parasitic capacitances are depicted in the enlarged subfigure.

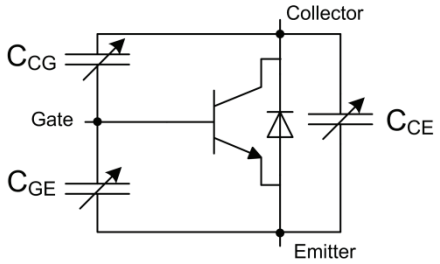

intrinsic parasitic capcitances	nF*)
C_{iss} (=C_{rss} +C_{GE})	8,3
C_{rss} (=C_{CG})	0,5
C_{oss} (=C_{CE}+ C_{rss})	1,2

*) V_{CE}=25V, T_{vj}=25°C, f=1MHz

Fig. 4 IGBT intrinsic parasitic capacitances

The dynamic characteristics of a power semiconductor switch (in this case IGBT) are influenced by several parasitic capacitances. The input capacitance is defined by the parallel connected gate-emitter C_{GE} and gate-collector C_{GC} capacitance, which are the basis for the adequate dimensioning of the gate driver circuit. The capacitance C_{GC} is also referred to as the reverse transfer capacitance C_{rss}. The output capacitance C_{oss} which is the sum of C_{GC} and C_{CE}, limits the dv/dt at the switching transition. Each time the semiconductor switch turns on, the energy stored in the output capacitance will be dissipated in the device. The output capacitance could be measured by setting a bias DC voltage between collector and emitter during gate-emitter is ac shorted with a capacitor. The value of C_{oss} at a DC voltage of $25V_{CE}$ results in 1nF. However, the value varies non-linearly as a function of the collector to emitter voltage. Thus, the value specified in the data sheet, representing a single value at one voltage level could not be used in any calculation that involves C_{oss}. At higher voltage levels, as they occur in the investigation of this work, the value is strongly decreasing to a value of several pF. Thus, the influence of the intrinsic capacitances is rather negligible. However, as the proposed monitoring method is implemented as a comparative method it is of vital of importance that the detected changes in the frequency range between the initially healthy machine and over years aged machine, are only occurring due to the winding insulation degradation affects. However, aging also occurs in the power semiconductor and it is intended to show how the impact can be tested on the insulation monitoring method. The various mechanical parts of the three phase bridge inverter module are expanded and contracted at different temperatures during the operation. This eventually produces cracking due to fatigue, which lower the critical capability of the bond to transfer heat generated in the die. In [17] and [18] an increase in the junction temperature *Tj* due to fatigue is accompanied by a reduced latch current, resulting in an increase of the transistor turn-off time. Investigations regarding the influences of the dv/dt-rise times of the excitation voltage on the proposed method are given in [19]. By varying the external gate resistor to influence the switching performance, realized with a voltage source inverter prototype equipped with SiC semi-conductors, a variation of the inverter output dv/dt-rate from 1kV/µs-20kV/µs is conducted. It was concluded that the proposed online insulation condition monitoring method is well working and applicable to inverter fed AC machines with different highly increased dv/dt-rates of the inverter output voltage. Additional investigations regarding the influences of external parasitic capacitances of the inverter are conducted in the next paragraphs.

In Fig. 5 (a) the inverter and the three half-bridge IGBT module are visible. To cause a change in the parasitic capacitance $C_{Inv\text{-}Gnd}$ an electrically insulating ground plate was added between the heat sink and the package. In the right subfigure (b) the capacitance over a wide frequency range is shown, measured between *L1* and ground potential at disconnected machine and cabling. The values decrease from the 'Inverter – initial state' from 730pF to 240pF by adding plates with different thickness.

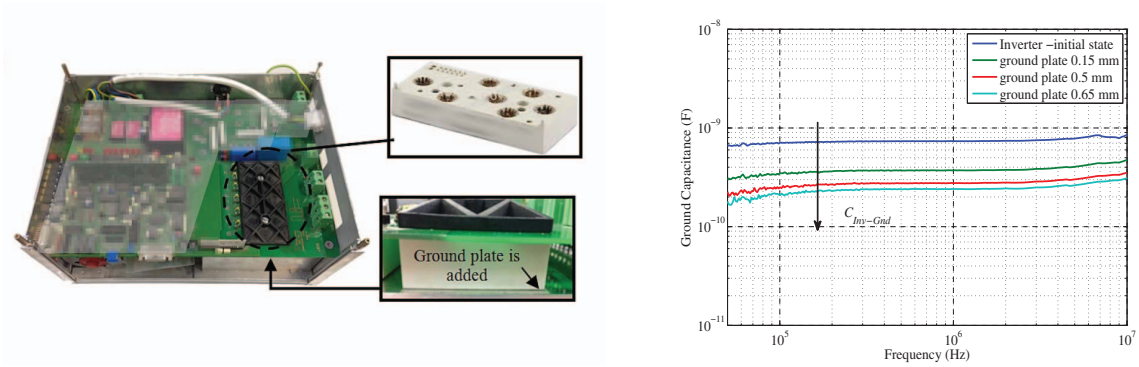

(a) (b)

Fig. 5 a) Test bench inverter, IGBT-module and additional ground plate b) Measured ground capacitance

The change in the inverter to ground capacitance is taken as a possible deviation in the inverter configuration and could be assessed as an aging phenomenon or resulting from semiconductor exchange. In Fig. 6 (a) the phase voltage measured from L1 to starpoint is visible for the healthy machine state and the inverter configuration 'Healthy - IGBT1' (blue trace) and the machine with emulated insulation degradation with 7.5nF parallel the first coil of phase L1 'Degraded – IGBT 1' is depicted (dotted red trace). In the lower subfigure the measurement of the healthy machine state with the initial inverter configuration and the configuration 'IGBT2' (green trace) with a ground plate of 0.65mm between IGBT package and heat sink is compared. The differences observable in the first comparison are visible in the low frequency part of the decaying oscillation, wherein the second comparison shows more deviations immediately after switching transition at higher frequencies.
In Fig. 6 (b) the corresponding current responses for the aforementioned test scenarios are shown. The deviation between 'Healthy – IGBT 1' and 'Degraded – IGBT 1' is clearly visible. However between the two converter configurations it is negligible.

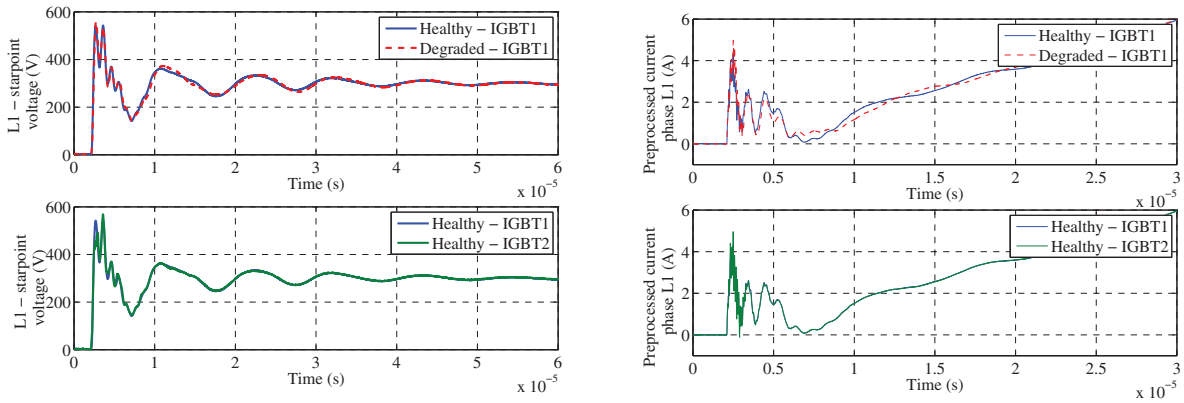

(a) (b)

Fig. 6 (a) L1 to starpoint voltage for different inverter configurations b) resulting current signals for machine and inverter degradation scenarios.

In Fig. 7 (a) the current signals are depicted after signal conditioning with elimination of the current slope to prevent influences through machine asymmetries (e.g. slotting), which contains no significant information for the insulation state estimation. The signals are truncated after 30µs with the start point at the first rising edge after inverter switching. By applying a rectangular window, the data is transferred into the frequency domain. The results are depicted in the upper and lower subfigure (b). The maximum deviation, approximately with a decrease of 50% of the initial value, was recorded for a frequency of about 150 kHz. A deviation of the spectra caused by a change of the inverter configuration was noticed for higher frequencies above 10 MHz. Thus, the frequency range for the evaluation of the insulation condition is limited up to 1 MHz. Additionally, this limit enables the usage

of low sampling ADC units in order to perform the insulation monitoring with economically acceptable conditions.

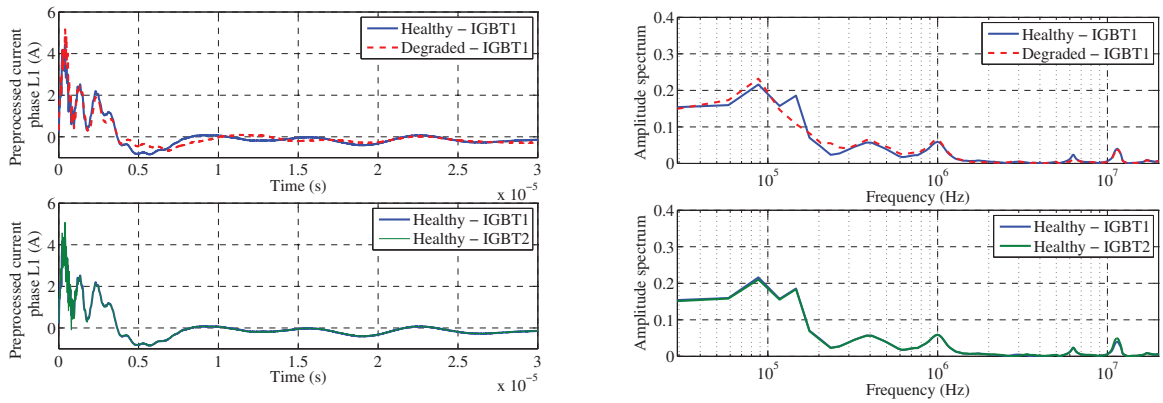

(a) (b)

Fig. 7 (a) Resulting current signals after signal processing b) corresponding spectra of the current signals.

In Fig. 8 (a) the calculated indicators for different scenarios concerning two converter scenarios and capacitor values parallel the winding system are depicted. An increase in the indicator by use of larger capacitors can be equated with an increasingly deteriorated insulation. This is equivalent to a change in the capacitance of the winding. In both cases, 'IGBT 1' as well as 'IGBT 2' the tested scenarios show monotonic increasing tendency with increasing capacitor values. The machine state 'Healthy – IGBT 1' serves as the reference and all further states are compared to this measurement (square deviation between equidistant frequency points of spectra in the frequency range up to 1MHz).

In Fig. 8 (b) the ground leakage current I_{GND} (cf. Fig. 1) flowing through ground connection between the motor and converter after voltage step excitation of phase L1 is depicted in the upper subfigure. The shape of the current is characterized by the equivalent impedance of the converter grounding connection $Z_{GND,\,C}$ as well as the impedance of the motor grounding connection $Z_{GND,M}$. The connection builds the largest loop and conducts the main leakage current. In this test setup the converter and machine are connected by unshielded three phase cables. In many typical drives the motor and converter are connected by shielded cables, which are also carrying leakage current flowing between machine and converter. The dc-link voltage is supplied by a constant dc power supply. In the lower subfigure, the spectrum components up to 1 MHz of the leakage current are depicted. The difference between the ‚Healthy – IGBT 1' and ‚Healthy – IGBT 2' are negligible.

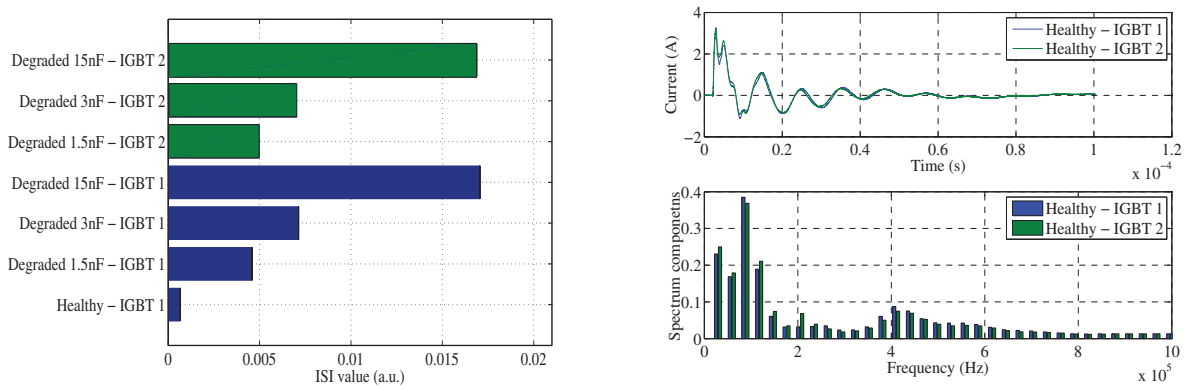

(a) (b)

Fig. 8 (a) L1 to starpoint voltage for different inverter configurations b) resulting indicators for machine and inverter degradation scenarios.

Conclusions

The aim of this paper is to demonstrate the feasibility of monitoring a change of the machine winding insulation respectively its insulation strength. With the proposed method detection of insulation degradation is realized by the current's transient evaluation after voltage step excitation with the inverter. The usage of the built-in current transducers is one of the key targets to safe space and costs for the system. The change of the parasitic machine winding capacitances influence the current transient response and a deviation of its frequency components within a defined range indicate that insulation degradation occurred. As the proposed monitoring method is implemented as a comparative method it is of vital of importance that the detected changes between the initially healthy machine and the same machine aged over years, are only stimulated due to the winding insulation degradation affects. With the presented investigations it can thus be concluded that the proposed insulation condition monitoring method is well working despite a possible change of the inverter configuration and is applicable to inverter-fed AC machines with different highly increased dv/dt-rates of the converter output voltage. Changes through parasitic capacitances from the inverter are negligible considering the performance of the insulation monitoring method.

References

[1] Stone, G. C.; Boulter, E. E.; Culbert, I. and Dhirani, H.; "Electrical Insuation for Rotating Machines". *IEEE Press*, 2004.

[2] IEEE "Recommended Practice for Measurement of Power Factor Tip-Up of Electric Machinery Stator Coil Insulation," *IEEE Std 286-2000* , pp.i,29, 2001.

[3] IEEE "Recommended Practice for Testing Insulation Resistance of Electric Machinery," *IEEE Std 43-2013*, pp.1,75, March 6 2014.

[4] Ahola, J.; Särkimäki, V,; Muetze A.; Tamminen J.; "Radio-frequency-based detection of electrical discharge machining bearing currents," *IET Electric Power Applications*, volume 5, issue 4, p. 386 – 392, 2011.

[5] Ait-Amar, S.; Roger, D,; "Prospective method for partial discharge detection in large AC machines using magnetic sensors in low electric field zones," *IET International Conference on Computation in Electromagnetics (CEM 2011)*, volume 5, issue 4, p. 386 – 392, 2011.

[6] Toliyat, Hamid A., et al. "Electric Machines: Modeling, Condition Monitoring, and Fault Diagnosis". *CRC Press*, 2012.

[7] Neti, P.; Grubic, S., "Online broadband insulation spectroscopy of induction machines using signal injection," *IEEE Energy Conversion Congress and Exposition (ECCE),* vol., no., pp.630,637, 14-18 Sept. 2014.

[8] Zoeller, C.; Vogelsberger, M.A.; Fasching, R.; Grubelnik, W.; Wolbank, Th.M., "Evaluation and current-response based identification of insulation degradation for high utilized electrical machines in railway application," *10th IEEE International Symposium on Diagnostics for Electrical Machines, Power Electronics and Drives (SDEMPED)*, pp.266-272, 2015.

[9] Farahani, M.; Gockenbach, E.; Borsi, H.; Schäfer, K.; Kaufhold, M.; "Behavior of machine insulation systeMHz subjected to accelerated thermal aging test," *IEEE Transactions on Dielectrics and Electrical Insulation,* vol.17, no.5, pp.1364-1372, 2010.

[10] Perisse, F.; Werynski, P.; Roger, D., "A New Method for AC Machine Turn Insulation Diagnostic Based on High Frequency Resonances," *IEEE Transactions on Dielectrics and Electrical Insulation*, vol.14, no.5, pp.1308,1315, October 2007.

[11] Oswald, N.; Anthony, P.; McNeill, N.; Stark, B.H., "An Experimental Investigation of the Tradeoff between Switching Losses and EMI Generation With Hard-Switched All-Si, Si-SiC, and All-SiC Device Combinations," *IEEE Transactions on Power Electronics*, vol.29, no.5, pp.2393-2407, May 2014.

[12] Nussbaumer, P.; Wolbank, T.M.; Vogelsberger, M.A., "Separation of disturbing influences on induction machine's high-frequency behavior to ensure accurate insulation condition monitoring," *28th IEEE Annual Applied Power Electronics Conference and Exposition (APEC)*, pp.1158,1163, 2013.

[13] Knockaert, J.; Peuteman, J.; Catrysse, J.; Belmans, R., "Hidden reflection phenomena on inverter-fed induction motors," *European Conference on Power Electronics and Applications*, pp.9 pp.-P.9, 11-14 Sept. 2005.

[14] Amarir, S.; Al-Haddad, K., "Mathematical analysis and experimental validation of transient over-voltage higher than 2 per unit along industrial ASDM long cables," *IEEE Power Electronics Specialists Conference*, pp.1846-1851, 15-19 June 2008.

[15] Muetze, A.; Binder, A., "Calculation of Circulating Bearing Currents in Machines of Inverter-Based Drive Systems," *IEEE Transactions on Industrial Electronics*, vol. 54, no. 2, pp. 932-938, April 2007.

[16] Said, A.; Al-Haddad, K.; "A new approach to analyze the overvoltages due to the cable lengths and EMI on adjustable speed drive motors," *IEEE Power Electronics Specialists Conference,* pp. 3964-3970 Vol.5., 2004.

[17] Patil, N.; Das, D.; Goebel, K.; Pecht, M., "Identification of failure precursor parameters for Insulated Gate Bipolar Transistors (IGBTs)," *International Conference on Prognostics and Health Management, (PHM),* pp.1-5, 2008.

[18] Brown, D.W.; Abbas, M.; Ginart, A.; Ali, I.N.; Kalgren, P.W.; Vachtsevanos, G.J., "Turn-Off Time as an Early Indicator of Insulated Gate Bipolar Transistor Latch-up," *IEEE Transactions on Power Electronics*, , vol.27, no.2, pp.479-489, 2012.

[19] Vogelsberger, M.A.; Zoeller, C.; Wolbank, Th.M.; Ertl, H., "Analysis of Ultra-fast Inverter Switching Transition (dv/dt) Impact based on SiC Semi-conductors to Pre-active Insulation Monitoring of High Power," *Proceedings of International Exhibition and Conference for Power Electronics, Intelligent Motion, Renewable Energy and Energy Management; PCIM Europe*, pp.1-7, 2015.